

PHYSICS AT FUTURE LINEAR COLLIDERS

Swathi Sasikumar

Max-Planck-Institute for Physics, Munich

Abstract

The International Linear Collider (ILC) and the Compact Linear Collider (CLIC) are the two proposed e^+e^- linear colliders operating at different centre-of-mass energies and with at least one of the beams polarised. The experiments at these facilities provide a platform to perform high-precision measurements of Standard Model observables and searches for new particles complimenting the HL-LHC programme. In this contribution, different studies of the two linear colliders are discussed. Experiments at linear e^+e^- colliders, with a relatively clean environment compared to hadron colliders, can perform precision measurements of electroweak and Higgs boson and top quark production processes. In this contribution, the focus is on the analysis of single Higgs production, double Higgs production, and top-Yukawa coupling.

1 Introduction

In the history of particle physics, e^+e^- colliders have played complementary roles in shedding light on to the properties of elementary particles. The prediction of top mass at LEP experiments had a key role in helping discover the top quark at Tevatron in the predicted mass range ^{1, 2)}. Similarly, the discovery of gluon at PETRA ^{3, 4)}, precise measurement of Z boson at LEP and the SLC ⁵⁾ have made very important contributions to particle physics. After the discovery of Higgs boson at the LHC experiments ⁶⁾, an e^+e^- collider can perfectly compliment the hadron collider to make precision measurements of the Higgs boson. Moreover, at higher energies, an e^+e^- collider can provide an environment to make precise measurements of top quark mass and understand top-Yukawa coupling as well as top-electroweak coupling.

The International Linear Collider (ILC) and Compact Linear Collider (CLIC) are two proposed e^+e^- linear colliders. The ILC is a 20 km (31 km for 500 GeV) machine which has a tunable centre-of-mass energy between 250-500 GeV (upgradable to 1 TeV) whereas the CLIC (50 km) can operate at a centre-of-mass energy of 380 GeV

to 3 TeV. Both the electron and positron beams are polarised for the ILC as $P(e^-) = \pm 80\%$ and $P(e^+) = \pm 30\%$. CLIC has its electron beam polarised to $\pm 80\%$. The schematic pictures of both the colliders are given in figure 1.

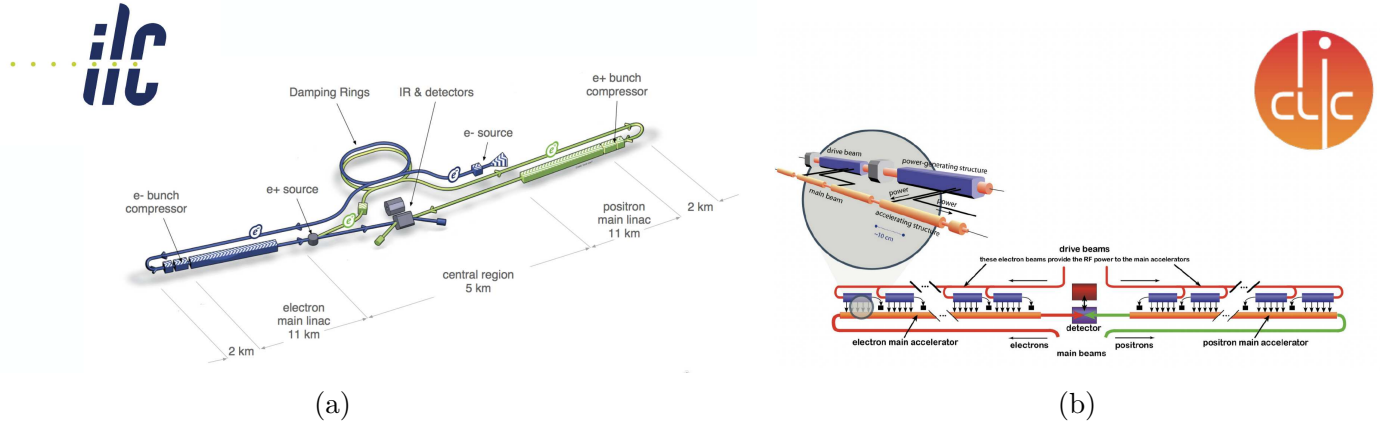


Figure 1: (a) The schematic design of the International Linear Collider for 500 GeV machine ⁷⁾. (b) The schematic design for the Compact Linear Collider ⁸⁾.

2 Advantages of a linear e^+e^- collider

Being an e^+e^- collider, ILC and CLIC mainly have electroweak production and therefore very clean physics environment. The significantly smaller amount of background allows a 'no trigger' policy on the events produced. This means, all the produced events can be included in the analysis and no sample is discarded. Moreover, the colliding particles being fundamental particles, e^+e^- colliders have a very well defined centre-of-mass energy of $\sqrt{s} = 2E_{beam}$. This allows the use of kinematic information and thus gives the opportunity to make model-independent measurements.

Linear colliders can provide access to a center-of-mass energy well above what can be reached in practical circular machines. Another important advantage of a linear collider is that the electron and positron beams can be polarised. Polarisation enables reducing the background and enhancing the signal as required. A detailed review of the benefits of beam polarisation for the physics reach of ILC can be found in ⁹⁾ and ¹⁰⁾.

3 Single Higgs Production

One of the most important analyses planned at the e^+e^- colliders is the Higgs analysis. The precise measurement of Higgs decay branching ratios is key to probing new physics in the Higgs sector. The e^+e^- colliders serve as a Higgs factory at a centre-of-mass energy of 250 GeV. Some of the important processes for the production of single Higgs can be seen in Fig. 2a. Single Higgs is produced mainly through higgstrahlung, gauge boson fusion, and top-Yukawa coupling. Higgstrahlung is found to be the dominant process around 250 GeV ¹¹⁾ whereas above 350 GeV processes like gauge boson fusion starts gaining significance.

The e^+e^- colliders have an initial state with well-defined four-momentum. This allows the identification of Higgs bosons in higgstrahlung process using the mass recoiling against an identified Z boson, without any reference to the decay products of the Higgs. At 250 GeV, ILC can produce up to half a million Higgs bosons that are completely unbiased with respect to Higgs decay. Using such a sample precise measurements of Higgs boson properties e.g. partial cross-section to different Higgs decay modes can be made. Some of these measurements

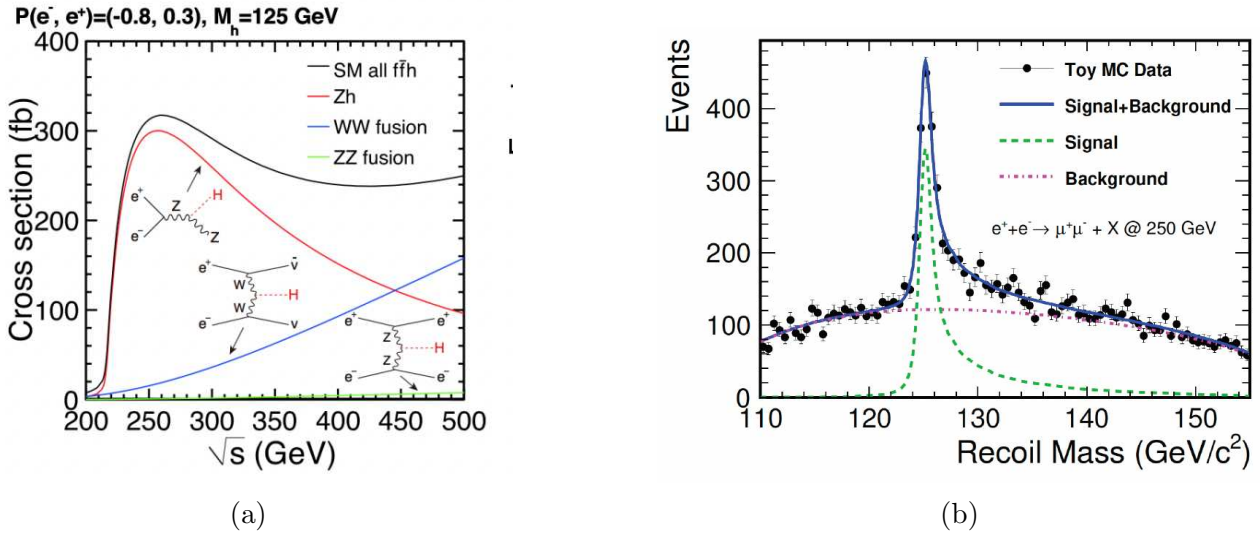


Figure 2: (a) Cross sections for major Higgs production processes as a function of center-of-mass energy ¹¹. (b) Recoil mass spectrum against $Z \rightarrow \mu^+\mu^-$ for signal $e^+e^- \rightarrow ZH$ and SM background at 250 GeV ¹².

strongly depend on the Higgs boson mass which can be measured very precisely using the recoil technique. Also, since the identification of the Higgs boson does not depend on the decay mode, it is also possible to measure the total higgstrahlung production cross-section at the ILC. The recoil mass is measured as:

$$m_{rec}^2 = (\sqrt{s} - E_Z)^2 - p_z^2 \quad (1)$$

where m_{rec} is the recoil mass, \sqrt{s} is the centre-of-mass energy, E_Z and p_z is the energy and momentum of the identified Z boson. The identified Z boson in a higgstrahlung event can decay to hadrons or to charged leptons. A study for the ILC showed that for a higgstrahlung process at $\sqrt{s} = 250$ GeV and a luminosity of 2 ab^{-1} where Z decays leptonically, the precision on the HZ cross-section can be achieved as $\Delta\sigma(HZ)/\sigma(HZ) = 1.0\%$ ¹². The higgstrahlung process where Z decays hadronically have a ten times higher cross-section than the leptonic decays ¹³. However, at 250 GeV, the HZ production is not far above the threshold and therefore the recoil mass distribution is relatively closer to the kinematic limit. This region is populated by processes like $e^+e^- \rightarrow qqqq$ (from $e^+e^- \rightarrow ZZ$ or $e^+e^- \rightarrow WW$) with large cross sections. Separation of signal from these backgrounds is very challenging especially when Higgs boson decays hadronically too. An analysis at CLIC shows the measurement of Higgs mass and precision on HZ cross section using higgstrahlung process at different centre-of-mass energies. This study shows that the best sensitivity for the precision study is obtained at 350 GeV since the HZ production is further from the threshold. This provides better separation of signal from the most challenging backgrounds. The summary of the statistical precision achievable on $\sigma(HZ)$ can be seen in table 1.

The Higgs mass can also be directly reconstructed from its decay products, providing complementary measurements. The majority of Higgs bosons decay hadronically, with the dominant branching fractions corresponding to $H \rightarrow b\bar{b}$, $H \rightarrow c\bar{c}$ and $H \rightarrow g\bar{g}$. The separation of these processes strongly relies on jet flavor tagging. The jet flavor tagging algorithm at ILC, called as LCFIplus, has achieved an excellent b- and c- tagging performance in full simulation studies of the ILD concept at ILC ¹⁶. At a centre-of-mass energy $\sqrt{s} = 250$ GeV and a nominal luminosity of 2 ab^{-1} , the application of the LCFIplus algorithm to the hadronically decaying Higgs boson allows the measurement of the partial cross-section $\sigma_{ZH} \times BR(H \rightarrow bb)$ to 0.7% and $\sigma_{ZH} \times BR(H \rightarrow cc, gg)$ to around 4 %

\sqrt{s} [GeV]	\mathcal{L}_{int} [fb $^{-1}$]	$\sigma(HZ)$ [fb]	$\Delta\sigma(ZH)$ [%]
250	1000	136	2.58
350	1000	93	1.27
420	1000	68	1.86

Table 1: The statistical precision achievable on $\sigma(HZ)$ for different centre-of-mass energies ¹³⁾.

precision both the major polarization combinations ¹⁵⁾. The identification of $H \rightarrow ss$ decays presents a significant challenge due to its subtle signature and small expected branching ratio.

For the processes where Higgs decays leptonically, the measurements can be performed if the branching ratios are similar to as predicted in the Standard Model. An ILC study for a centre-of-mass energy 250 GeV showed that the partial cross-section $\sigma(ZH) \times \text{BR}(H \rightarrow \tau\tau)$ can be measured with a precision less than 2% ¹⁷⁾. However, for the $\mu\mu$ decay of Higgs, the small branching ratio of $H \rightarrow \mu\mu$ limits the statistics available at ILC. Nevertheless, the partial cross-section $\sigma(ZH) \times \text{BR}(H \rightarrow \mu\mu)$ can still be measured with a precision of 17% for combined 250 GeV and 500 GeV results ¹⁸⁾.

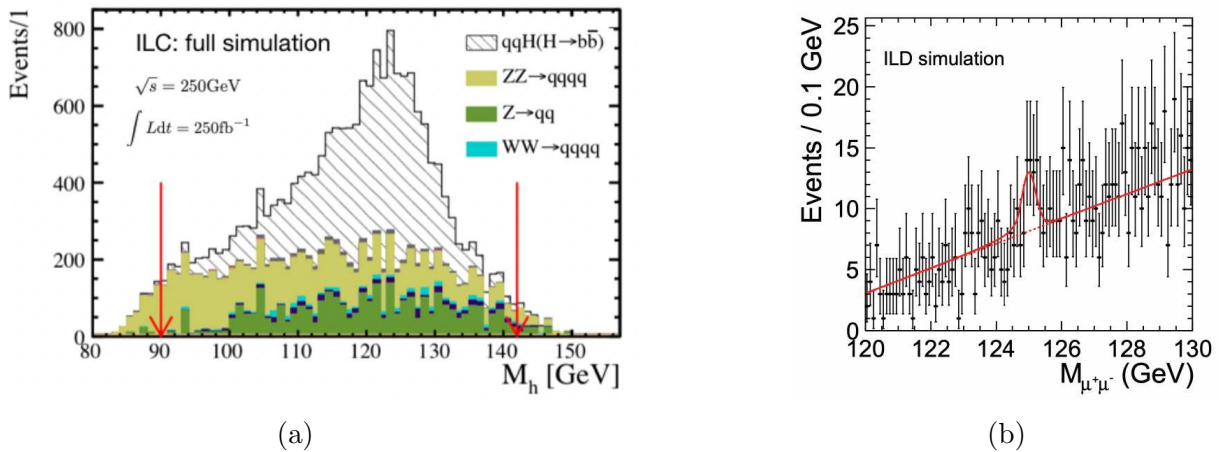


Figure 3: (a) Comparison of signal and backgrounds from ILD full simulation for the measurement of the $\sigma \times \text{BR}$ for $H \rightarrow b\bar{b}$, for 250 fb^{-1} of ILC data at 250 GeV ¹⁶⁾. (b) Data from pseudo-experiment fitted by a Gaussian to extract its mean and width ¹⁸⁾

4 Di-Higgs production at linear lepton colliders

At a centre-of-mass energy of at least 500 GeV, the self-interaction of the Higgs boson, particularly, the triple Higgs coupling λ , can be probed directly by analysing the Higgs boson pairs. The di-Higgs production at e^+e^- colliders happen through two important processes e.g. $e^+e^- \rightarrow ZHH$ (double higgstrahlung) and $e^+e^- \rightarrow \nu\bar{\nu}HH$ (WW fusion). The cross-section for these processes as a function of the centre-of-mass energies can be seen in figure 4a.

The prospects of measuring double Higgs production through these two reactions have been studied at the ILC for data fully simulated for the ILD detector. These studies were conducted both for $\sqrt{s} = 500 \text{ GeV}$ ¹⁹⁾ and $\sqrt{s} = 1 \text{ TeV}$ ²⁰⁾. It was found that, if the Higgs self-coupling value stays as that predicted by the Standard

Model, then the double higgstrahlung can be observed at a centre-of-mass energy of 500 GeV with a significance of 8σ combining the $HH \rightarrow b\bar{b}b\bar{b}$ and $HH \rightarrow b\bar{b}WW^*$ channels. This results in the measurement of λ with a precision of 27%. With the improvements in the detector that are relevant for these measurements and with the inclusion of $HH \rightarrow \tau^+\tau^-b\bar{b}$ it has been estimated that the precision on λ can be improved to 21-22% ¹⁹⁾. Also, the inclusion of double Higgs production from WW fusion at 1 TeV can improve the relative precision on λ to 10%.

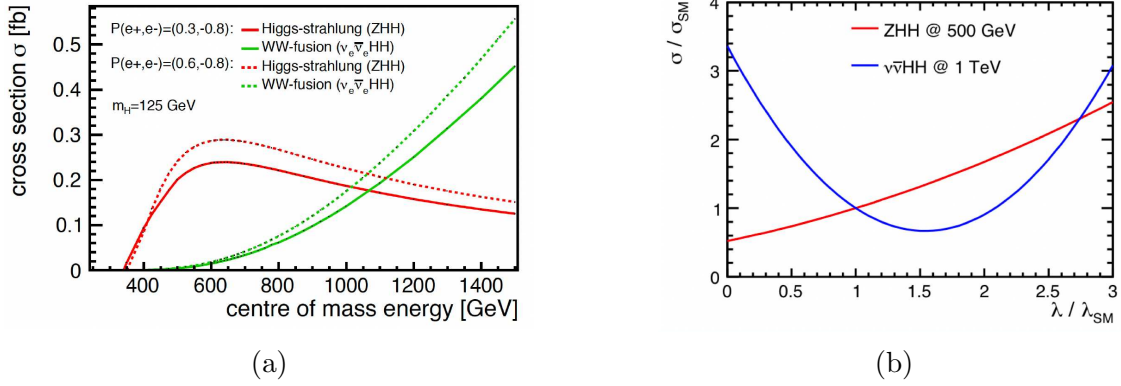


Figure 4: (a) Double-Higgs production cross sections of ZHH and WW fusion as a function of centre-of-mass energies for two different beam polarisation. (b) Precision of production cross sections for WW fusion and double higgstrahlung as a function of Higgs self-coupling λ normalised to λ_{SM} ²¹⁾

The most important benefit of an e^+e^- collider that can operate at a centre-of-mass energy of 500 GeV and above is that both the double Higgs production processes can be obtained. This is significant in the case where the value of λ is different from that predicted by the Standard Model. The precision of the production cross sections for WW fusion and double higgstrahlung as a function of Higgs self-coupling λ normalised to λ_{SM} is given in figure 4b. As can be seen, the cross-section for ZHH increases with an increase in triple Higgs coupling (λ) whereas the cross-section for the WW fusion process decreases. If the Higgs self-coupling deviates from the Standard Model, the two channels would interfere with the Standard Model effects. At the ILC, no matter which signs λ turns out to be, one of the possible reactions will increase in cross-section and reflect this improved sensitivity.

At proton colliders, this is however not the case. The dominant double Higgs production $gg \rightarrow HH$ is a fusion process with destructive interference. And the double Higgstrahlung process has a very small cross-section as compared to e^+e^- colliders. Therefore, unlike at the ILC, LHC can only have one process to measure the self-coupling. The ILC on the other hand can guarantee a measurement of the self-coupling at the level of at least 30% for whatever the value of self-coupling actually might be, combining the results from two different channels complimentary to each other. Figure 5 shows the impact of this synergy as compared to an extrapolation of the uncertainty projections from the ATLAS collaboration ²²⁾ to non-Standard Model values of λ .

5 Top Quark Mass

The top quark mass is one of the important fundamental measurements to be experimentally determined. Direct measurements of top quark mass at hadron colliders could reach a precision of 600 MeV at the LHC ^{26, 27)} and Tevatron ²⁸⁾. Whereas, the top quark mass measurements at HL-LHC are expected to reach an experimental precision of a few hundred MeV ²⁹⁾. An electron-positron collider that can produce top quark pairs has an excellent potential to measure the top quark mass with even better precision. Several studies of top threshold scan have

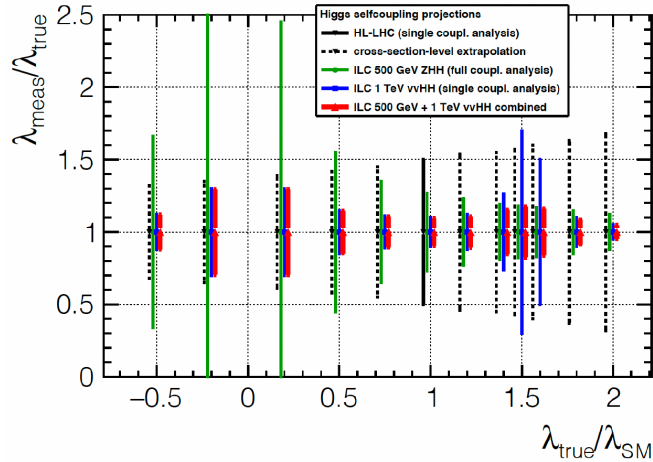


Figure 5: Expected uncertainties in the determination of the Higgs self-coupling at the HL-LHC and the ILC as a function of λ/λ_{SM} [19, 22].

been performed by several groups [30, 31, 32, 33]. A simulated scan of top quark threshold in [30] is shown in Figure 6.

A statistical uncertainty of ~ 30 MeV was estimated in a study performed at CLIC with the $l+jets$ channel with an integrated luminosity of 500 fb^{-1} at $\sqrt{s} = 380 \text{ GeV}$ [30].

6 Top Yukawa Coupling

The top quark is the particle that has the strongest coupling to the Higgs boson. Therefore it is very important to understand why the top-Yukawa coupling is the strongest among all the others. At the ILC, both direct and indirect probe of the top quark is possible. The main processes to access top quark at ILC are $e^+e^- \rightarrow t\bar{t}$ at $2m_t$, $e^+e^- \rightarrow t\bar{t}H$ and $e^+e^- \rightarrow t\bar{t}\nu_e\bar{\nu}_e$. The $t\bar{t}$ threshold scan offers an indirect measurement of top Yukawa coupling with a precision of 4% [23]. To measure the top-Yukawa coupling directly, it is required that the centre-of-mass energy is at least 500 GeV. With a rise of the centre-of-mass energy further to 550 GeV the cross-section for $t\bar{t}H$ rises sharply by a factor of ~ 4 and the measurement of $t\bar{t}H$ coupling by a factor of two. Several studies have been performed on this for centre-of-mass energies ranging from 500 GeV - 1.4 TeV [23, 24, 25]. For a centre-of-mass energy of 550 GeV and a nominal luminosity of 4 ab^{-1} , the top-Yukawa coupling can be measured with a precision of 2.8 %. With the increase in the centre-of-mass energy to 1 TeV and the luminosity to 8 ab^{-1} , the precision improves to 1 %.

7 Conclusion

This paper gives a very brief review of different kinds of studies at e^+e^- linear colliders, mainly for the studies conducted at the ILC. It can be seen that substantial improvements with respect to the hadron colliders are possible at the ILC for the discussed topics. Precise measurements of single Higgs and Higgs self-coupling are possible where especially the model-independent approach gives better possibilities. Along with precision measurements, a search for new particles in the electroweak scale may also be possible at the ILC.

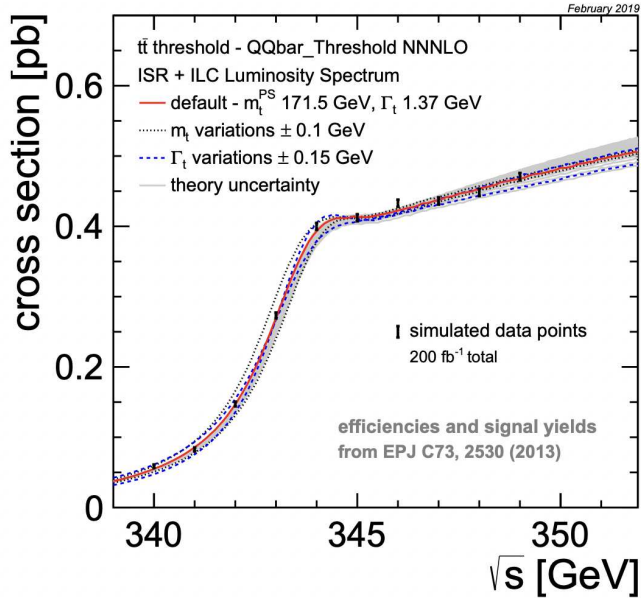


Figure 6: A simulated top quark threshold scan with an integrated luminosity of 200 fb^{-1} . The bands around the central cross section curve show the dependence of the cross section on the top quark mass and width [30].

References

1. Abe, F. Observation of Top Quark Production in $\bar{p}p$ Collisions with the Collider Detector at Fermilab. *Phys. Rev. Lett.* **74**, 2626-2631 (1995,4), <https://link.aps.org/doi/10.1103/PhysRevLett.74.2626>.
2. Abachi, S. Observation of the Top Quark. *Phys. Rev. Lett.* **74**, 2632-2637 (1995,4), <https://link.aps.org/doi/10.1103/PhysRevLett.74.2632>.
3. Barber, D. Discovery of Three-Jet Events and a Test of Quantum Chromodynamics at PETRA. *Phys. Rev. Lett.* **43**, 830-833 (1979,9), <https://link.aps.org/doi/10.1103/PhysRevLett.43.830>.
4. Al, C. Evidence for gluon bremsstrahlung in ee annihilations at high energies. *Physics Letters B* **86**, 418-425 (1979), <https://www.sciencedirect.com/science/article/pii/0370269379908694>.
5. The ALEPH Collaboration, The DELPHI Collaboration, The L3 Collaboration, The OPAL Collaboration, The SLD Collaboration, The LEP Electroweak Working Group, Electroweak, T. & Groups, H. Precision Electroweak Measurements on the Z Resonance. *Physics Reports* **427**, 257-454 (2006,5), <http://arxiv.org/abs/hep-ex/0509008>, arXiv: hep-ex/0509008.
6. Aad, G. Combined Measurement of the Higgs Boson Mass in pp Collisions at $\sqrt{s} = 7$ and 8 TeV with the ATLAS and CMS Experiments. *Phys. Rev. Lett.* **114**, 191803 (2015,5), <https://journals.aps.org/prl/abstract/10.1103/PhysRevLett.114.191803>.
7. Adolphsen, C. The International Linear Collider Technical Design Report - Volume 3.II: Accelerator Baseline Design. *ArXiv:1306.6328 [physics]*. (2013,6), <http://arxiv.org/abs/1306.6328>, arXiv: 1306.6328.

8. Linssen, L., Miyamoto, A., Stanitzki, M. & Weerts, H. Physics and Detectors at CLIC: CLIC Conceptual Design Report. (arXiv,2012), <https://arxiv.org/abs/1202.5940>.
9. Fujii, K. The role of positron polarization for the initial 250 GeV stage of the International Linear Collider. *ArXiv:1801.02840 [hep-ex, Physics:hep-ph]*. (2018,1), <http://arxiv.org/abs/1801.02840>, arXiv: 1801.02840.
10. Moortgat-Pick, G. The role of polarized positrons and electrons in revealing fundamental interactions at the Linear Collider. *Physics Reports*. **460**, 131-243 (2008,5), <http://arxiv.org/abs/hep-ph/0507011>, arXiv: hep-ph/0507011.
11. Baer, H., Barklow, T., Fujii, K., Gao, Y., Hoang, A., Kanemura, S., List, J., Logan, H., Nomerotski, A., Perelstein, M., Peskin, M., Pöschl, R., Reuter, J., Riemann, S., Savoy-Navarro, A., Servant, G., Tait, T. & Yu, J. The International Linear Collider Technical Design Report - Volume 2: Physics. *ArXiv:1306.6352 [hep-ph]*. (2013,6), <http://arxiv.org/abs/1306.6352>, arXiv: 1306.6352.
12. Yan, J., Watanuki, S., Fujii, K., Ishikawa, A., Jeans, D., Strube, J., Tian, J. & Yamamoto, H. Measurement of the Higgs boson mass and $e^+e^- \rightarrow ZH$ cross section using $Z \rightarrow \mu^+\mu^-$ and $Z \rightarrow e^+e^-$ at the ILC. *Phys. Rev. D*. **94**, 113002 (2016).
13. Thomson, M. A. Model-independent measurement of the $e^+e^- \rightarrow HZ$ cross section at a future e^+e^- linear collider using hadronic Z decays. *Eur. Phys. J. C*. **76**, 72 (2016), <https://doi.org/10.1140/epjc/s10052-016-3911-5>.
14. Aryshev, A. The International Linear Collider: Report to Snowmass 2021. (arXiv,2022), <https://arxiv.org/abs/2203.07622>.
15. Ono, H. & Miyamoto, A. A study of the measurement precision of the Higgs boson branching ratios at the International Linear Collider. *Eur. Phys. J. C*. **73**, 2343 (2013).
16. The ILD Collaboration International Large Detector: Interim Design Report. (arXiv,2020), <https://arxiv.org/abs/2003.01116>.
17. Kawada, Shin-ichi, Fujii, Keisuke, Suehara, Taikan, Takahashi, Tohru & Tanabe, Tomohiko A study of the measurement precision of the Higgs boson decaying into tau pairs at the ILC. *Eur. Phys. J. C*. **75**, 617 (2015), <https://doi.org/10.1140/epjc/s10052-015-3854-2>.
18. Kawada, Shin-ichi, List, Jenny & Berggren, Mikael Prospects of measuring the branching fraction of the Higgs boson decaying into muon pairs at the International Linear Collider. *Eur. Phys. J. C*. **80**, 1186 (2020), <https://doi.org/10.1140/epjc/s10052-020-08729-7>.
19. Duerig, C. Measuring the Higgs self-coupling at the International Linear Collider.(2016).
20. Tian, J. Study of Higgs self-coupling at the ILC based on the full detector simulation at $\sqrt{s} = 500$ GeV and $\sqrt{s} = 1$ TeV. *3rd Linear Collider Forum*. pp. 224-247 (2013).
21. Higgs Projections using the ILD at the ILC, Junping Tian, ALCW15.
22. Measurement prospects of the pair production and self-coupling of the Higgs boson with the ATLAS experiment at the LH-LHC, ATLASCollaboration.

23. Yonamine, R., Ikematsu, K., Tanabe, T., Fujii, K., Kiyo, Y., Sumino, Y. & Yokoya, H. Measuring the top Yukawa coupling at the ILC at $\sqrt{s}=500$ GeV. *Phys. Rev. D* **84** pp. 014033 (2011)
24. Abramowicz, H. & Others Higgs physics at the CLIC electron–positron linear collider. *Eur. Phys. J. C* **77**, 475 (2017).
25. Price, T., Roloff, P., Strube, J. & Tanabe, T. Full simulation study of the top Yukawa coupling at the ILC at $\sqrt{s}=1$ TeV. *Eur. Phys. J. C* **75**, 309 (2015).
26. Aaboud, M. et al. Measurement of the top quark mass in the $t\bar{t} \rightarrow$ lepton+jets channel from $\sqrt{s}=8$ TeV ATLAS data and combination with previous results. *Eur. Phys. J. C* **79**, 290 (2019).
27. ATLAS, T., CDF, CMS & D0 Collaborations First combination of Tevatron and LHC measurements of the top-quark mass. *ArXiv E-prints*. pp. earXiv:1403.4427 (2014,3).
28. Tevatron Electroweak Working Group, T. & Aaltonen, T. Combination of CDF and D0 results on the mass of the top quark using up 9.7 fb^{-1} at the Tevatron. (2016,8).
29. Azzi, P. & Al. Standard Model Physics at the HL-LHC and HE-LHC. (2019,2).
30. Zarnecki, A. Top-quark physics at CLIC. *PoS. EPS-HEP2019* pp. 626 (2020).
31. Seidel, K., Simon, F., Tesar, M. & Poss, S. Top quark mass measurements at and above threshold at CLIC. *Eur. Phys. J. C* **73**, 2530 (2013).
32. Horiguchi, T., Ishikawa, A., Suehara, T., Fujii, K., Sumino, Y., Kiyo, Y. & Yamamoto, H. Study of top quark pair production near threshold at the ILC. (2014).
33. Martinez, M. & Miquel, R. Multiparameter fits to the t anti-t threshold observables at a future e+ e- linear collider. *Eur. Phys. J. C* **27** pp. 49-55 (2003).